Science Essence Journal Vol. 42 No. 1 (2026) | 50-70

Research Article

Computational Analysis of FDA-Approved Drugs for Potential Repurposing in Alzheimer's Disease: Targeting mTOR and NGFR Pathways

Narudol Teerapattarakan[1], Phateep Hankittichai[1,2], Shisanupong Anukanon[1]*

Received: 5 August 2025
Revised: 21 September 2025
Accepted: 30 September 2025

ABSTRACT

Alzheimer's disease (AD) remains a significant unmet medical challenge. This study investigates the repurposing of FDA-approved drugs for AD using computational methods. From 4,046 screened drugs, 341 candidates were retained based on pharmacokinetic criteria, including blood–brain barrier permeability and gastrointestinal absorption. Molecular docking identified nandrolone phenylpropionate, atovaquone, and cholecalciferol as top candidates for mTOR, and nandrolone phenylpropionate, ethynodiol diacetate, and drospirenone for p75 neurotrophin receptor (p75NTR). Molecular dynamics simulations assessed the stability of these protein-ligand complexes, revealing that atovaquone and ethynodiol diacetate exhibited the highest stability with mTOR and p75NTR, respectively. Despite the promising binding properties of steroid-based drugs, their systemic side effects necessitate further structural modifications. This study demonstrates the feasibility of drug repurposing for AD and underscores the importance of computational approaches in accelerating the discovery of new therapeutic options.

Keywords: Drug repurposing, Mammalian target of rapamycin, Nerve growth factor receptor, Alzheimer's disease, Computational analysis.

[1] School of Medicine, Mae Fah Luang University, Chiang Rai 57100, Thailand

[2] Cancer and Immunology Research Unit (CIRU), School of Medicine, Mae Fah Luang University, Chiang Rai 57100, Thailand

*Corresponding author, email: shisanupong.anu@mfu.ac.th

Introduction

Alzheimer's disease (AD) represents a significant challenge in neurodegenerative research, primarily characterized by progressive cognitive decline and memory loss, severely impacting patients' quality of life and imposing a significant burden on caregivers and healthcare systems [1]. The pathogenesis of AD has been widely explained through two dominant hypotheses: the amyloid hypothesis and the tau hypothesis. The amyloid hypothesis posits that AD is initiated by the overproduction and accumulation of amyloid-beta (Aβ) peptides in neurons, disrupting normal brain function and leading to neurodegeneration [2]. Conversely, the tau hypothesis suggests that the excessive phosphorylation of tau proteins results in unstable microtubules, forming neurofibrillary tangles that impede normal neuronal activity [3]. Despite extensive research, no approved therapies have effectively modified these pathological features or altered disease progression. Current therapeutic approaches for AD primarily focus on symptomatic relief, with acetylcholinesterase inhibitors and NMDA receptor antagonists being the main classes of drugs used. These treatments temporarily alleviate cognitive symptoms by enhancing neurotransmitter function but do not halt or reverse the underlying neurodegenerative processes [1, 2]. The lack of disease-modifying therapies highlights the urgent need for novel strategies to prevent neuronal loss and brain atrophy in AD [4].

One promising target in AD research is the mammalian target of rapamycin (mTOR), a protein complex vital for numerous cellular processes and metabolic functions [5]. The activation of mTOR inhibits autophagy, leading to the aggregation of amyloid proteins and the phosphorylation of tau proteins, which are central to AD pathology [6, 7]. Consequently, the development of mTOR inhibitors presents a promising avenue for AD treatment.

Another potential therapeutic target is nerve growth factor (NGF), a polypeptide hormone that influences neuronal growth and survival [8]. The NGF receptor (NGFR) is crucial for the development and maintenance of cholinergic neurons, which are significantly affected in AD [9]. Studies suggest that NGF can inhibit mTOR activity, thereby potentially reducing the accumulation of Aβ peptides and the hyperphosphorylation of tau proteins [10, 11]. By modulating mTOR activity, NGF not only supports neuronal survival but also mitigates key pathological processes associated with both the amyloid and tau hypotheses [12].

The traditional drug development process faces challenges such as evolving regulatory requirements, which increase research costs and extend development timelines [2]. An alternative strategy is drug repurposing, which involves identifying new therapeutic uses for existing drugs [14]. This approach leverages the established safety profiles of these drugs, reducing the risk of research failure, shortening development time, and lowering costs [13, 14]. Computational methods, such as molecular docking and molecular dynamics, enable the rapid assessment of drug-target interactions, identifying candidates that may inhibit Aβ production or tau phosphorylation.

This study employs molecular docking to screen FDA-approved drugs using computer simulations to predict their interactions with mTOR and NGFR. In addition to molecular docking, computational pharmacokinetic predictions are utilized to assess the ability of these drugs to cross the

blood-brain barrier (BBB). This step is crucial in narrowing down the list of potential drugs by ensuring that only those capable of effectively reaching the brain are considered for further analysis [15]. By integrating knowledge from chemistry, biochemistry, computer-aided drug design, pharmacology, and medical sciences, this research aims to identify potential drugs for repurposing to treat AD in the elderly. This comprehensive approach not only enhances the efficiency of identifying viable therapeutic candidates but also contributes significantly to the development of disease-modifying therapies.

Materials and Methods

In this study, we explored the potential of repurposing existing drugs for Alzheimer's disease (AD) treatment using a computational approach. The method involved several key steps, as summarized in Figure 1.

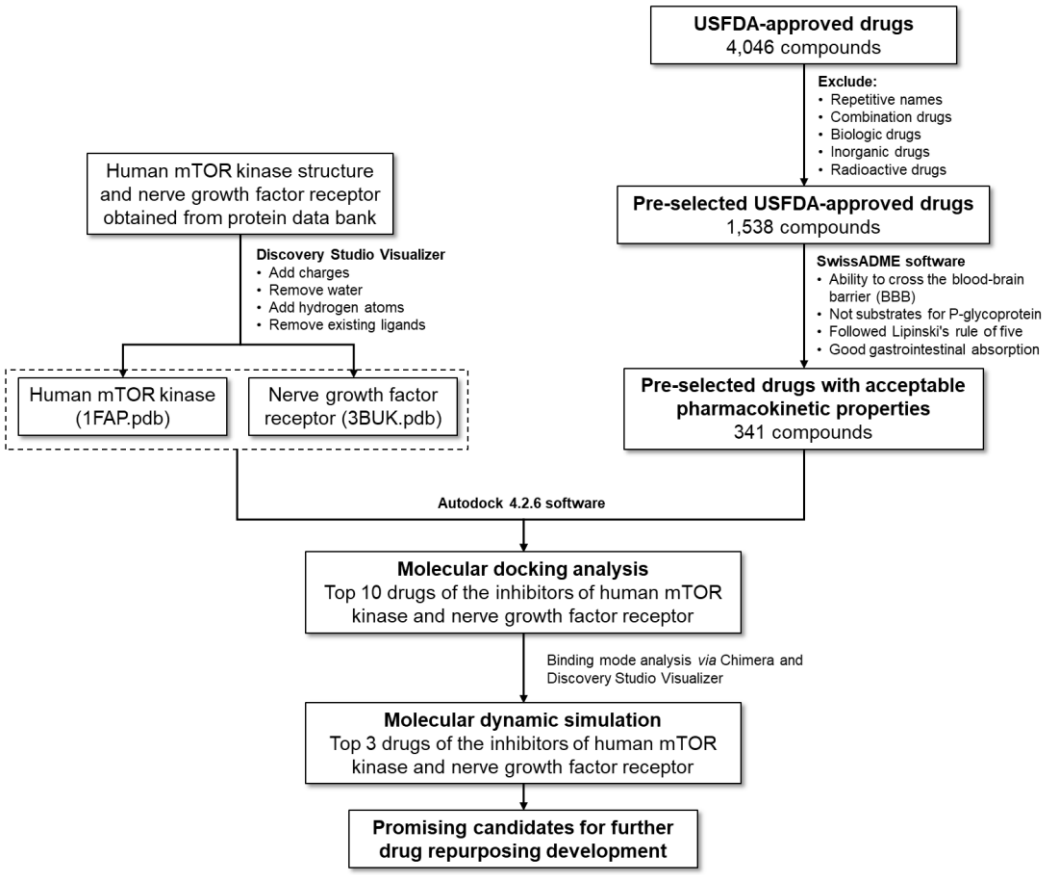

Figure 1 Research methodology using computational software for repurposing in Alzheimer's disease treatment.

Collection and preparation of FDA-approved drugs

The sample for the *in silico* study comprises all FDA-approved drugs, totaling 4,046 drugs, sourced from the FDA Drug Database from https://www.accessdata.fda.gov/scripts/cder/daf/index.cfm?event=browseByLetter.page&productLetter=A&ai=0. The chemical structures of these drugs were drawn

using ChemDraw Professional 16.0 and converted into the Simplified Molecular Input Line Entry System (SMILES) format for subsequent computational analysis.

Computational pharmacokinetic analysis

The SMILES files of all drug structures were subjected to computational pharmacokinetic analysis using SwissADME. This tool calculates key physicochemical properties of small drug molecules, including molecular weight (MW), number of heavy atoms, number of rotatable bonds, number of hydrogen bond acceptors (HA), number of hydrogen bond donors, polar surface area (PSA), lipophilicity, and water solubility. Additionally, it evaluates crucial pharmacokinetic properties such as gastrointestinal absorption, blood-brain barrier (BBB) permeability, P-glycoprotein substrate properties, and cytochrome P450 (CYP) inhibitors properties (CYP1A2, CYP2C19, CYP2C9, CYP2D6, CYP3A4) [16].

To select drugs for the next steps, several criteria were applied: adherence to Lipinski's rules (ensuring the drugs are orally active), the ability to pass the blood-brain barrier (necessary for targeting the brain in AD treatment), good gastrointestinal absorption, non-substrate properties for *P*-glycoprotein (to avoid drug efflux), and absence of cytochrome P450 (CYP) inhibitors properties (CYP1A2, CYP2C19, CYP2C9, CYP2D6, CYP3A4) [17]. These criteria ensure that only drugs with favorable pharmacokinetic profiles and the potential for effective central nervous system activity are considered for further analysis.

Molecular docking analysis

Target proteins associated with AD in this study, the mammalian target of rapamycin (mTOR) and nerve growth factor receptors (NGFR), were obtained from the Protein Data Bank (PDB) with the respective codes 1FAP and 3BUK [18, 19]. To prepare these crystal structures for docking simulations, all water molecules, solvents, and co-crystallized ligands were meticulously removed to ensure a clean and accurate environment for further analysis.

The calculated binding free energy and inhibitory constant of the selected drugs were analyzed using AutoDock 4.2.6 software [20]. Initially, each drug candidate was subjected to energy minimization to attain the most stable conformations, reducing potential steric clashes and internal strain. Ligand energy minimization was performed using Chem3D Professional 10.0 with the MM2 force field to eliminate steric clashes and obtain optimal conformations prior to docking.

Docking grids were defined to cover the known or predicted functional binding pockets of each target [9, 21]. Grid maps were generated with AutoGrid4 using a spacing of 0.375 Å and box dimensions of 60×60 × 60 points, ensuring adequate coverage of active site residues. The Lamarckian Genetic Algorithm (LGA) was employed with the following parameters: population size = 150, maximum energy evaluations = 2.5×10^6, maximum generations = 27,000, mutation rate = 0.02, crossover rate = 0.8, elitism = 1, and local search iterations = 300 with a pseudo-Solis & Wets algorithm (local search frequency = 0.06). For each ligand–target pair, 100 independent docking runs (ga_run = 100) were performed to ensure statistical robustness. Docked conformations were clustered at an RMSD tolerance

of 2.0 Å. The most populated cluster (Cluster 1) was considered the dominant binding mode, with its mean binding energy (ΔG ± SD) and occupancy (%) recorded. The lowest binding energy (best ΔG) and corresponding inhibition constant (K_i) were also reported.

Reference ligands (Sirolimus for mTOR; NSC49652 for NGFR; Donepezil as a clinically approved drug for AD) were used to benchmark our docking–MD pipeline by comparing their scores and stability metrics with those of the screened candidates. These controls provided pharmacological context and internal validation of parameterization and analysis workflows.

Molecular dynamic simulation

The top four docked complexes were selected for molecular dynamics (MD) simulations, conducted with GROMACS 5.1.4 (www.gromacs.org/) [22]. The CHARMM36 force field was applied to the protein and membrane, while the ligands were parameterized using the Charmm General Force Field (CGenFF). Van der Waals interactions were handled using a dual cutoff approach, with inner and outer cutoffs set at 10 Å and 12 Å, respectively. The Particle–Mesh–Ewald (PME) method was used for calculating long-range electrostatic interactions. Hydrogen atoms were constrained using the LINear Constraint Solver (LINCS) algorithm, and periodic boundary conditions were implemented. A time step of 2 fs was used throughout the simulations [23].

Initially, a 5000-step energy minimization was executed using the steepest-descent method to rectify steric clashes and eliminate any bad contacts in the initial structure, ensuring the system's stability. This was followed by equilibration under a constant volume and temperature (NVT) ensemble, with the temperature set to 310K using the Berendsen thermostat. During this phase, position restraints were applied to the protein and ligand to allow the solvent to relax around the fixed solutes. This NVT equilibration was carried out for 100 ps with a time step of 2 fs. Subsequently, the system underwent further equilibration under constant pressure and temperature (NPT) ensemble conditions. The Berendsen barostat was employed to maintain the pressure at 1 atm, allowing the system's density to stabilize. The same position restraints were kept, and this NPT equilibration also lasted for 100 ps with a time step of 2 fs.

After equilibration, production MD simulations were performed as independent replicates. Starting from the same equilibrated structure after NPT equilibration, different random velocity seeds (e.g., 11111, 22222, and 33333) were applied, yielding three independent 10-ns trajectories for each protein–ligand complex. This approach provided statistically independent replicates to enhance reproducibility. Trajectory analyses included root-mean-square deviation (RMSD) of protein and ligands, root-mean-square fluctuation (RMSF) of protein residues, radius of gyration (Rg), ligand–protein hydrogen bonds, and minimum distance between ligand and protein.

Statistical analysis

For each descriptor (ligand RMSD, protein RMSD, radius of gyration, and minimum distance), values from the equilibrated window (3–10 ns) were averaged per replicate and summarized as mean ±

SD across three independent runs. Trajectory data from 3–10 ns of the production phase were selected for statistical comparison, excluding the initial equilibration period (0–2 ns) during which the system undergoes conformational adjustments. This strategy ensured that only equilibrated dynamics were analyzed, thereby providing a reliable representation of protein–ligand stability and allowing statistically robust comparisons among ligands [24]. Normality was assessed using the Shapiro–Wilk test (all groups, $p > 0.05$), and homogeneity of variances was examined using the Brown–Forsythe test. When assumptions were satisfied, one-way ANOVA with Tukey's post-hoc test was applied; if variance heterogeneity was detected, Welch's ANOVA with Games–Howell post-hoc test was used as a robust alternative. All analyses were conducted in GraphPad Prism 9 with statistical significance set at $p < 0.05$.

Results and discussion

Drug repurposing, also known as drug repositioning, has gained significant attention in recent years due to its numerous advantages over traditional drug development processes [13]. One of the primary benefits is the substantial reduction in cost and time required to bring a drug to market. Since repurposed drugs have already been tested for safety and efficacy, they can bypass many early-stage clinical trials, which significantly shortens the development timeline and cuts research and development expenses [15]. In this study, the computational screening of FDA-approved drugs for potential repurposing in AD treatment involved rigorous analysis and multi-step methodologies.

The study focused on identifying drugs capable of interacting with critical targets: mammalian target of rapamycin (mTOR) and nerve growth factor receptor (NGFR). Molecular docking was utilized to predict binding affinities, and pharmacokinetic analyses ensured that drugs could cross the blood-brain barrier (BBB) and possessed favorable absorption profiles. This approach identified several promising candidates that exhibit strong interactions with mTOR and p75NTR of NGFR, essential proteins implicated in AD pathology.

Computational pharmacokinetic analysis of FDA-approved drugs

From an initial pool of 4,046 FDA-approved drugs, combination drugs, radioactive drugs, and inorganic drugs were excluded. This filtering process resulted in 1,538 remaining drugs, which were then subjected to comprehensive pharmacokinetic analysis using SwissADME. The criteria for selecting suitable drugs for AD treatment development were prioritized as follows: 564 drugs from the initial 1,538 had the ability to cross the blood-brain barrier (BBB); 356 of these 564 drugs were not substrates for *P*-glycoprotein; 339 of these 356 drugs followed Lipinski's rule of five; and 341 of these 343 drugs demonstrated good gastrointestinal absorption. Following this rigorous analysis, 341 drugs were identified as suitable candidates for further development in this study. These drugs were further evaluated for their binding affinity to target proteins, as detailed in Tables 1 and 2.

Table 1 Molecular docking analysis of the top 10 drugs with the best-calculated binding free energy for the protein 1FAP.

	Drug name	Best predicted ΔG (kcal/mol)[a]	K_i (nM)[b]	Cluster 1 mean ΔG±SD (kcal/mol)[c]	Cluster 1 occupancy (%)[d]
1	Nandrolone phenpropionate	-11.53	3.52	-11.11	63
2	Atovaquone	-11.15	6.67	-11.12	100
3	Cholecalciferol	-10.42	23.12	-9.78	44
4	Nefazodone	-10.34	26.48	-9.47	13
5	Rimonabant	-10.10	39.74	-10.32	5
6	Cyproheptadine	-10.01	46.24	-10.01	100
7	Droperidol	-10.00	46.56	-9.32	14
8	Quinestrol	-9.87	57.97	-9.88	3
9	Rimexolone	-9.82	63.41	-9.78	72
10	Ethynodiol diacetate	-9.81	64.10	-9.52	87
11	Sirolimus[e]	-9.82	63.71	-9.24	58
12	Donepezil[f]	-7.90	1,590	-3.79	18

[a] ΔG values are expressed in kcal/mol and were obtained using AutoDock 4.2.6 with the Lamarckian Genetic Algorithm (LGA).

[b] K_i values were empirically estimated from binding free energies as implemented in AutoDock.

[c] Cluster 1 mean ΔG±SD was calculated from all docking poses grouped within an RMSD tolerance of 2.0 Å.

[d] Cluster 1 occupancy indicates the proportion of docking runs (out of 100) that converged into the dominant binding cluster.

[e] Sirolimus was used as a reference mTOR inhibitor for comparative docking.

[f] Donepezil was included as a clinically approved Alzheimer's drug reference.

Molecular docking analysis of selected drugs to mTOR

The mTOR protein, one of the target proteins for AD drug development in this study, was obtained from the Protein Data Bank with the code 1FAP [18]. The SMILES files of all 341 selected drugs were studied for their binding affinity to the target protein, evaluating binding free energy and dissociation constant (K_d) using AutoDock 4.2.6 software. The binding site sphere radius of ligand-target interaction was fixed at 60 Å, covering the serine/threonine-protein kinase domain of the mTOR protein, based on previous studies focusing on critical residues TYR26, ARG42, LYS44, PRO45, MET49, VAL55, HIS87, SER125, ARG126, ARG132, and ARG199 [21].

Table 2 Molecular docking analysis of the top 10 drugs with the best-calculated binding free energy for the protein 3BUK.

	Drug name	Best predicted ΔG (kcal/mol)[a]	K_i (nM)[b]	Cluster 1 mean ΔG±SD (kcal/mol)[c]	Cluster 1 occupancy (%)[d]
1	Nandrolone phenpropionate	-12.04	1.51	-11.33	62
2	Ethynodiol diacetate	-10.93	9.78	-10.54	77
3	Drospirenone	-10.77	12.80	-10.50	100
4	Nefazodone	-10.68	14.96	-9.68	12
5	Azelastine	-10.68	14.77	-10.38	30
6	Progesterone	-10.62	16.47	-10.54	44
7	Flavoxate	-10.39	24.38	-10.27	4
8	Norgestimate	-10.32	27.13	-10.03	56
9	Testolactone	-10.28	29.27	-10.26	78
10	Sulfinpyrazone	-10.19	34.20	-10.16	12
11	NSC49652[e]	-9.93	52.72	-9.18	57
12	Donepezil[f]	-7.42	3,610	-7.12	7

[a] ΔG values are expressed in kcal/mol and were obtained using AutoDock 4.2.6 with the Lamarckian Genetic Algorithm (LGA).

[b] K_i values were empirically estimated from binding free energies as implemented in AutoDock.

[c] Cluster 1 mean ΔG±SD was calculated from all docking poses grouped within an RMSD tolerance of 2.0 Å.

[d] Cluster 1 Occupancy indicates the proportion of docking runs (out of 100) that converged into the dominant binding cluster.

[e] NSC49652 was used as a reference p75 neurotrophin receptor (p75NTR) agonist for comparative docking.

[f] Donepezil was included as a clinically approved Alzheimer's drug reference.

The docking analysis against mTOR revealed that nandrolone phenpropionate maintained the strongest binding affinity with a best ΔG of −11.53 kcal/mol (K_i = 3.52 nM) and a cluster mean ΔG of −11.11±SD kcal/mol, although its occupancy was moderate (63%). Atovaquone, despite having a slightly weaker predicted ΔG (−11.15 kcal/mol), showed 100% cluster occupancy, indicating a highly consistent binding mode across docking runs. In contrast, cholecalciferol displayed a best ΔG of −10.42 kcal/mol with lower cluster stability (occupancy 44%).

Interestingly, nefazodone, ranked fourth, exhibited a binding affinity (ΔG = −10.34 kcal/mol, K_i = 26.48 nM) comparable to the top three drugs, but its cluster occupancy was only 13%, suggesting

multiple alternative binding poses. Other compounds, including cyproheptadine (−10.01 kcal/mol), showed 100% occupancy, implying a highly stable conformation despite weaker binding affinity.

For comparative references, sirolimus (rapamycin), a known mTOR inhibitor, showed a binding energy of −9.82 kcal/mol with moderate occupancy (58%), while donepezil, a clinically approved Alzheimer's drug, bound weakly (ΔG = −7.9 kcal/mol, K_i = 1,590 nM) with low stability (occupancy 18%). These results validate the docking protocol by providing pharmacological benchmarks: sirolimus performed as expected within the inhibitory range, and donepezil confirmed its limited role in targeting mTOR.

In this study, the binding modes of the top 3 drugs with the best binding affinities to the mTOR protein were analyzed. These drugs include nandrolone phenylpropionate, atovaquone, and cholecalciferol, which displayed strong interactions and favorable binding free energies. Nandrolone phenylpropionate binding mode included a key hydrogen bond with VAL55, π-π T-shaped interactions with residues TYR26 and PHE2039, and π-alkyl interactions with residues TYR2105, TRP59, and TRP2101 (Figure 2a). Atovaquone exhibited several notable interactions with the mTOR protein. Conventional hydrogen bonds were observed with residues GLU54, VAL55, and ILE56, indicating strong polar interactions. Additionally, π-π T-shaped interactions were identified with residues PHE2108 and TYR2105. Alkyl interactions were also significant, involving LEU2031 and PHE2108, while π-alkyl interactions were noted with residues TRP2101, PHE2039, and PHE2108 (Figure 2b). Cholecalciferol primarily interacted with the mTOR protein through alkyl and π-alkyl interactions. The key residues involved included LEU2031, PHE46, TYR2105 and TRP59 for alkyl interactions, and TRP2101, PHE2108, ILE56, and VAL55 for π-alkyl interactions (Figure 2c).

Binding mode analysis indicated that the ligands aligned with key residues in the mTOR binding pocket, supporting their stability. Nandrolone phenylpropionate and atovaquone align in the same conformation, which is favorable for interaction with mTOR, resulting in the strongest binding free energies. In contrast, cholecalciferol does not align in the same conformation, indicating that this alignment is crucial for achieving strong binding affinities.

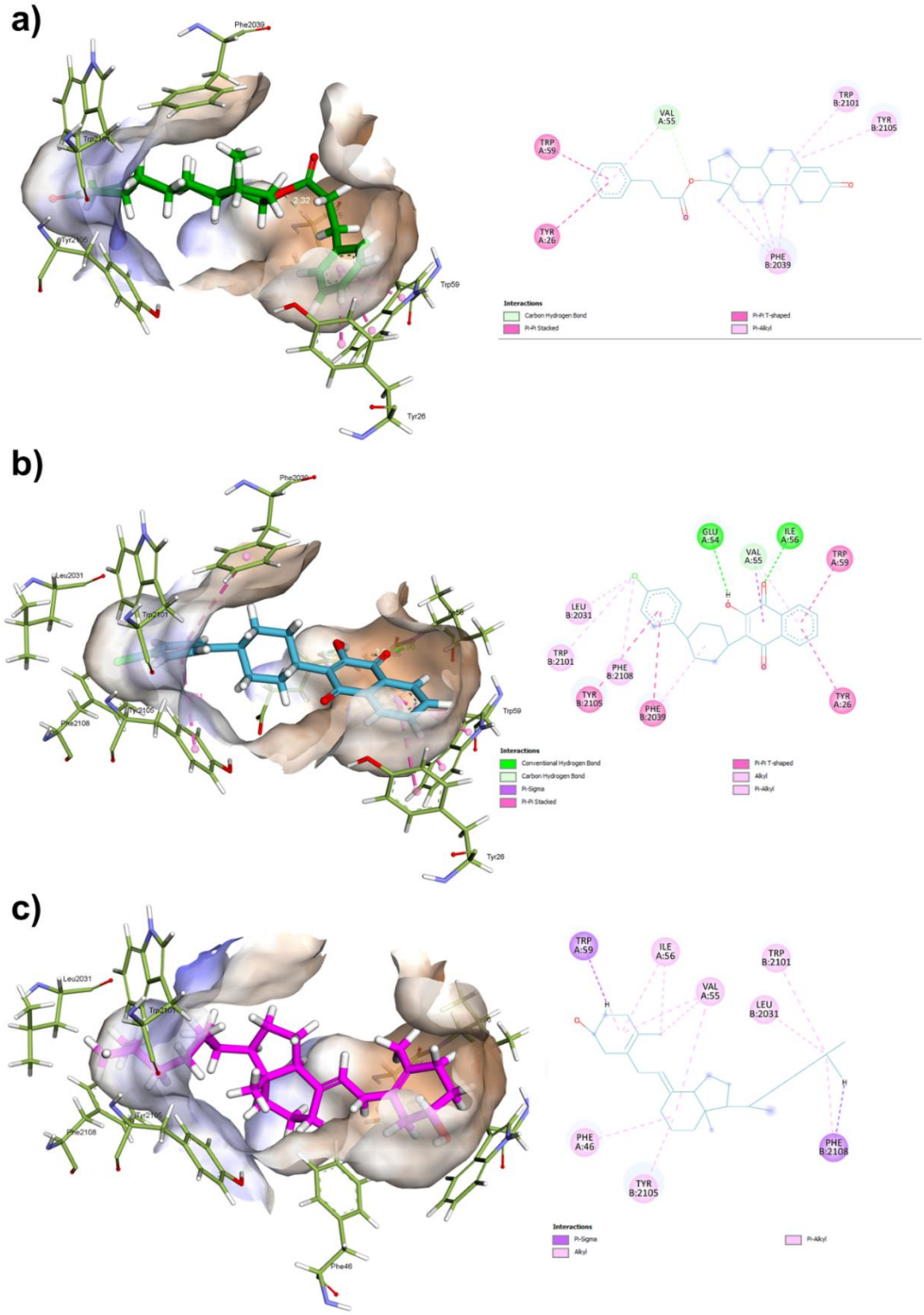

Figure 2 Binding modes of the top three drugs with the mTOR protein (1FAP): a) Nandrolone phenpropionate, b) Atovaquone, c) Cholecalciferol. Green dashed lines represent hydrogen bonds (Discovery Studio Visualizer).

Molecular docking analysis of selected drugs to p75 neurotrophin receptor

The Neurotrophin-3 (NT-3) and p75 neurotrophin receptor (p75NTR) complex, was obtained from the Protein Data Bank with the code 3BUK [19]. The binding affinities of 341 selected drugs to the p75NTR were analyzed using AutoDock 4.2.6 software. The binding affinities were evaluated by considering the key amino acids involved in the binding process. These amino acids were reported within broad ranges, ensuring a comprehensive analysis of the drug interactions [9].

Docking results against the p75NTR receptor similarly identified nandrolone phenpropionate as the top binder (ΔG = −12.04 kcal/mol, K_i = 1.51 nM), with a cluster mean ΔG of −11.33 kcal/mol and occupancy of 62%. Ethynodiol diacetate and drospirenone followed closely, with ΔG values of −10.93 kcal/mol and −10.77 kcal/mol, respectively, both showing stable clustering (occupancies of 77% and 100%). Among the additional candidates, nefazodone again demonstrated strong binding (−10.68 kcal/mol), although its cluster occupancy remained low (12%). azelastine and progesterone also ranked within the top six, but their cluster occupancies were moderate (30% and 44%).

As expected, the reference agonist NSC49652 bound with moderate affinity (ΔG = −9.93 kcal/mol, K_i = 52.72 nM) and an occupancy of 57%, consistent with its reported role as a p75NTR modulator. In comparison, donepezil showed a weak binding profile (ΔG = −7.42 kcal/mol, K_i = 3,610 nM, occupancy 7%), further confirming its lack of direct activity on this receptor.

Nandrolone phenpropionate shows strong interactions with p75NTR primarily through hydrogen bonds and hydrophobic interactions. The structural visualization indicates that nandrolone phenpropionate forms hydrogen bonds with key residues such as LYS71. These hydrogen bonds are crucial for stabilizing the ligand within the binding pocket. Additionally, nandrolone phenpropionate engages in π-alkyl interactions with residues like ILE73, CYS183, and MET125. These hydrophobic interactions further stabilize the ligand, ensuring a specific and robust binding to the protein (Figure 3a).

Ethynodiol diacetate interacts with p75NTR through a variety of interactions. It forms key hydrogen bonds with ASP128 and THR127, which are critical for maintaining the ligand within the active site. These hydrogen bonds provide significant stabilization, ensuring the ligand is securely anchored. Additionally, the attractive charge interaction with ASP128 enhances the binding affinity, reinforcing the stability of the ligand-protein complex. The combination of hydrogen bonding and electrostatic interactions provides a robust mechanism for the binding of ethynodiol diacetate, indicating its potential efficacy as an inhibitor (Figure 3b).

Drospirenone also shows strong interactions with p75NTR, facilitated through several key interactions. It forms significant hydrogen bonds with residues such as ASP104 and LYS71, which play a vital role in securing the ligand within the binding site. The hydrophobic interactions with residues like LEU173, ILE48, and VAL56 further enhance the binding stability. Additional carbon hydrogen bonds contribute to the overall stability and specificity of the ligand binding (Figure 3c).

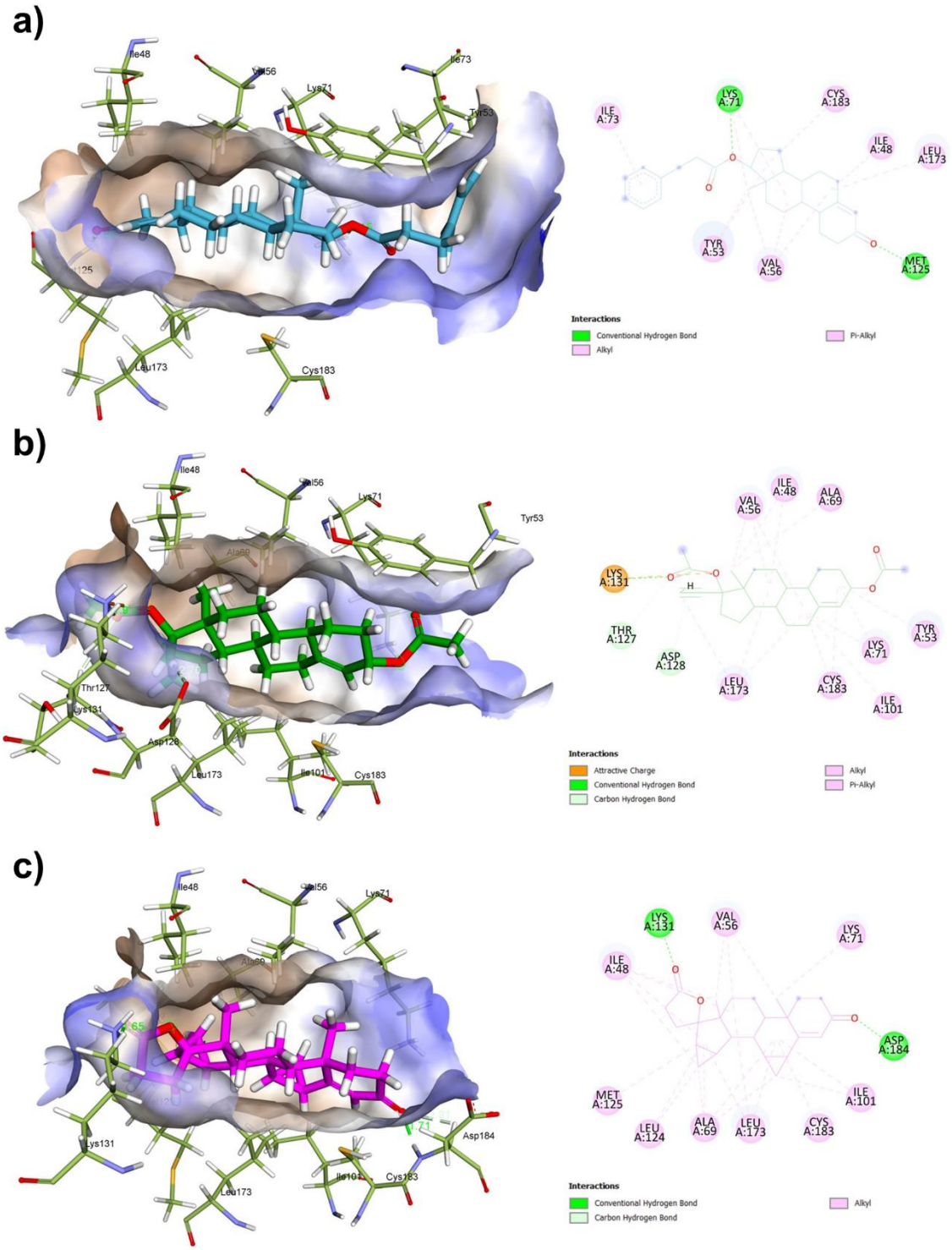

Figure 3 Binding modes of the top three drugs with the p75 neurotrophin receptor (p75NTR, 3BUK) a) Nandrolone phenpropionate, b) Ethynodiol diacetate, c) Drospirenone. Green dashed lines represent hydrogen bonds (Discovery Studio Visualizer).

Molecular dynamics analysis of selected drugs

The molecular dynamics (MD) simulations provided critical insights into the stability and conformational behavior of the top-ranking compounds against both the mTOR protein (1FAP) and the p75 neurotrophin receptor (p75NTR, 3BUK). These analyses extended beyond docking predictions by evaluating the dynamic stability of ligand–protein complexes using multiple descriptors, including root mean square deviation (RMSD), root mean square fluctuation (RMSF), radius of gyration (Rg), hydrogen bond formation, and minimum protein–ligand distance.

All datasets passed the Shapiro–Wilk normality test (p = 0.30–0.95). Most systems also satisfied homogeneity of variance by Brown–Forsythe test; however, one case (cholecalciferol with mTOR) showed significant variance heterogeneity. Accordingly, Welch's ANOVA with Games–Howell correction was applied for that dataset, whereas standard one-way ANOVA with Tukey's post-hoc test was used elsewhere. These adjustments ensured that all parametric analyses were valid.

For the mTOR complexes (1FAP), atovaquone emerged as the most stable candidate, maintaining the lowest RMSD values (~0.1 Å) throughout the 10 ns trajectory. Cholecalciferol and nandrolone phenpropionate exhibited moderate stability (~0.2 Å), whereas sirolimus, included as a reference mTOR inhibitor, showed slightly higher deviations but remained within 0.25 Å. By contrast, nefazodone displayed pronounced instability, with fluctuations reaching 0.5 Å, while donepezil, a clinically approved AD drug used as a reference, demonstrated only modest stability (Figure 4a-b). Ligand RMSD analyses supported these findings, showing that atovaquone and sirolimus remained firmly anchored within the binding pocket, while nefazodone and donepezil fluctuated more substantially (Figure 5a-b).

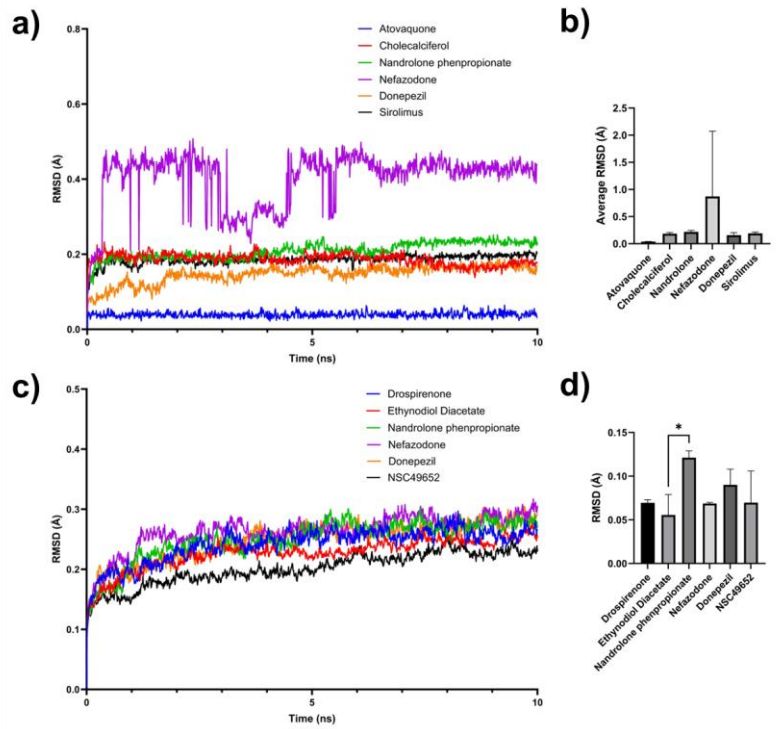

Figure 4 Protein RMSD of mTOR (1FAP) and p75NTR (3BUK) complexes during 10 ns MD simulations. (a, c) RMSD trajectories of 1FAP and 3BUK in complex with selected ligands. (b, d) Average RMSD values

(3–10 ns). Bars represent mean±SD. Statistical significance was determined by one-way ANOVA with Tukey's post-hoc test (*p < 0.05, **p < 0.01, ***p < 0.001), or by Welch's ANOVA with Games–Howell correction when variance homogeneity was violated (e.g., cholecalciferol in mTOR). Absence of asterisks indicates no significant difference.

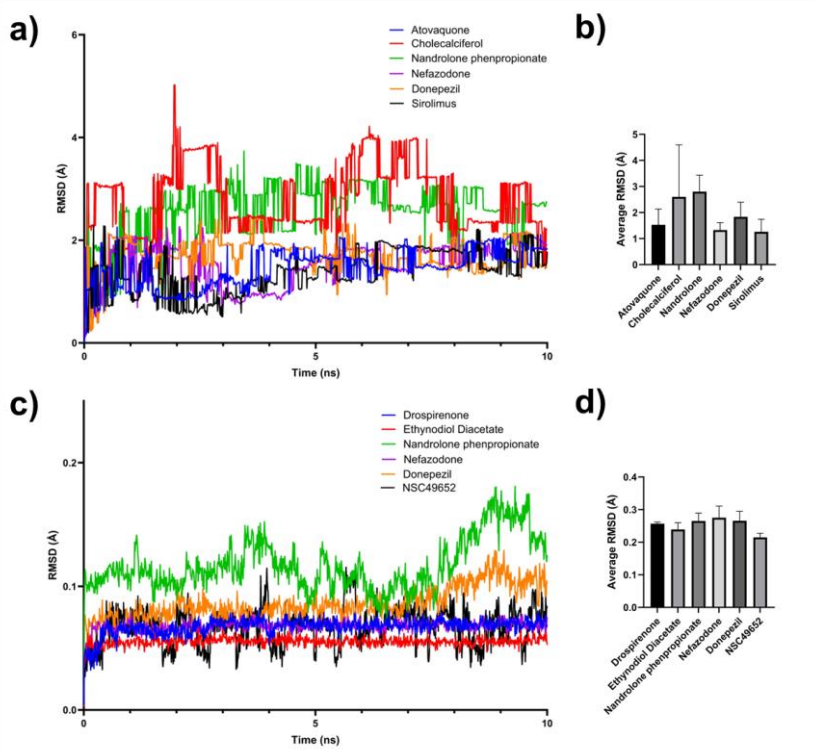

Figure 5 Ligand RMSD of mTOR (1FAP) and p75NTR (3BUK) complexes during 10 ns MD simulations. (a, c) RMSD trajectories of 1FAP and 3BUK in complex with selected ligands. (b, d) Average ligand RMSD values (3–10 ns). Bars represent mean±SD. Statistical significance was determined by one-way ANOVA with Tukey's post-hoc test (*p <0.05, **p < 0.01, ***p < 0.001), or by Welch's ANOVA with Games–Howell correction when variance homogeneity was violated (e.g., cholecalciferol in mTOR). Absence of asterisks indicates no significant difference.

The RMSF profiles revealed that most ligands induced minimal flexibility across the mTOR backbone, with only minor fluctuations localized to loop regions. Atovaquone and sirolimus complexes displayed consistently lower fluctuations, while nefazodone and donepezil induced higher local flexibility, consistent with their reduced stability (Figure 6a). Analysis of the radius of gyration (Rg) confirmed that the overall compactness of the protein was preserved across all simulations (~3.0–3.5 nm). Atovaquone and sirolimus maintained the most compact structures, while nandrolone phenpropionate and cholecalciferol caused slight increases in protein flexibility (Figure 7a-b).

Hydrogen bond profiling further differentiated these ligands: nefazodone consistently formed the highest number of hydrogen bonds (3–5 on average), reflecting strong polar interactions despite its unstable RMSD. Sirolimus also formed stable hydrogen bonds (~2–3) (Figure 8a). In contrast, atovaquone, nandrolone

phenpropionate, cholecalciferol, and donepezil formed fewer than 2 H-bonds on average. Statistical analysis (Tukey's multiple comparisons test) confirmed that nefazodone and sirolimus had significantly higher H-bond counts compared with other ligands ($p < 0.01$) (Figure 8b).

Minimum distance analyses supported ligand binding stability. Atovaquone maintained the closest average contact (~0.16 nm), significantly tighter than nefazodone (~0.22 nm) and nandrolone phenpropionate (~0.21 nm). Sirolimus also displayed stable interactions (~0.18 nm). Statistical comparisons indicated that atovaquone and sirolimus are bound significantly closer to the active site than nefazodone and cholecalciferol ($p < 0.05$) (Figure 9a-b).

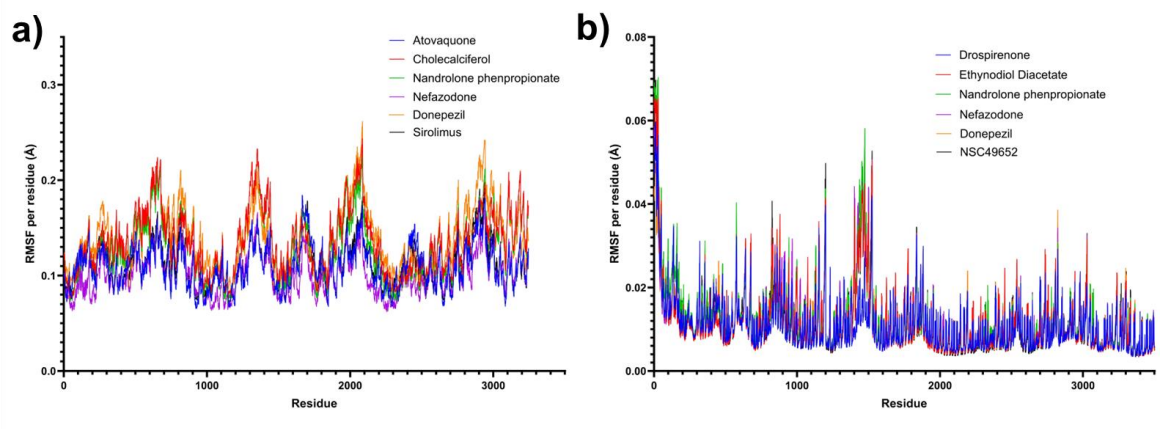

Figure 6. Protein RMSF of mTOR (1FAP) and p75NTR (3BUK) complexes during 10-ns MD simulations. (a) RMSF per residue of 1FAP in complex with selected ligands. (b) RMSF per residue of 3BUK in complex with selected ligands.

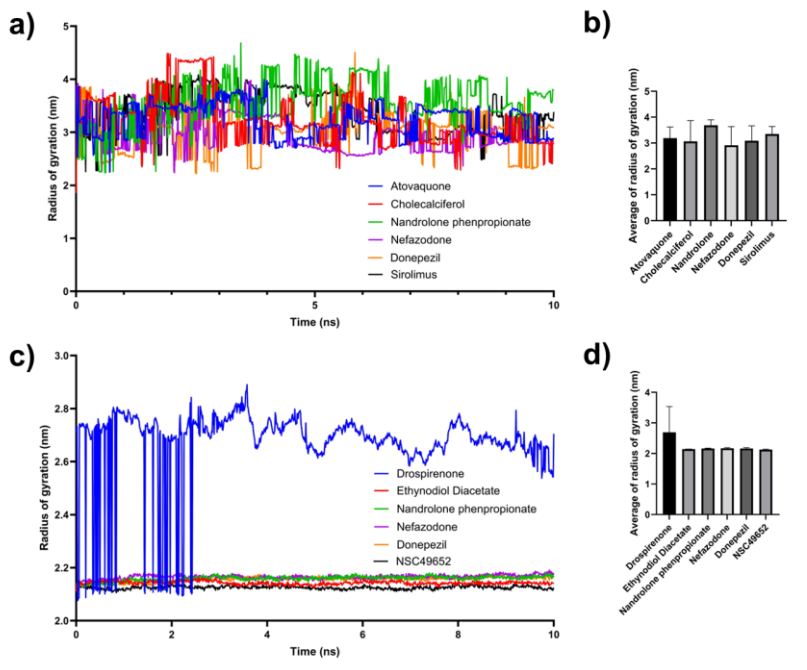

Figure 7. Radius of gyration (Rg) of mTOR (1FAP) and p75NTR (3BUK) complexes during 10 ns MD simulations. (a, c) Rg trajectories of 1FAP and 3BUK in complex with selected ligands. (b, d)

Average Rg values (3–10 ns). Bars represent mean ± SD. Statistical significance was determined by one-way ANOVA with Tukey's post-hoc test (*p < 0.05, **p < 0.01, ***p < 0.001), or by Welch's ANOVA with Games–Howell correction when variance homogeneity was violated (e.g., cholecalciferol in mTOR). Absence of asterisks indicates no significant difference.

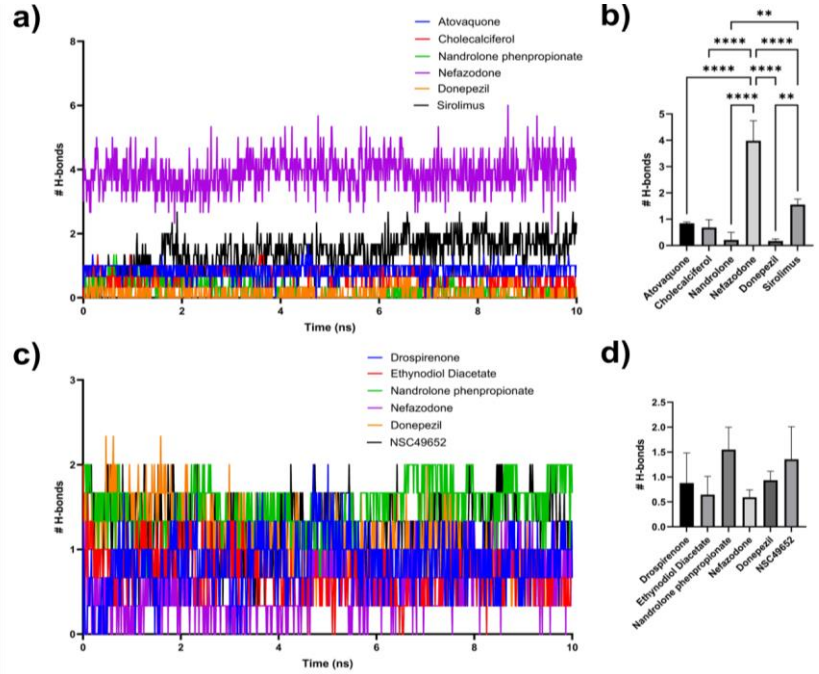

Figure 8. Hydrogen bonding profiles of mTOR (1FAP) and p75NTR (3BUK) complexes during 10 ns MD simulations. (a, c) Number of ligand–protein hydrogen bonds in 1FAP and 3BUK complexes. (b, d) Average hydrogen bond counts (3–10 ns). Bars represent mean±SD. Statistical significance was determined by one-way ANOVA with Tukey's post-hoc test (*p < 0.05, **p < 0.01, ***p < 0.001). Absence of asterisks indicates no significant difference.

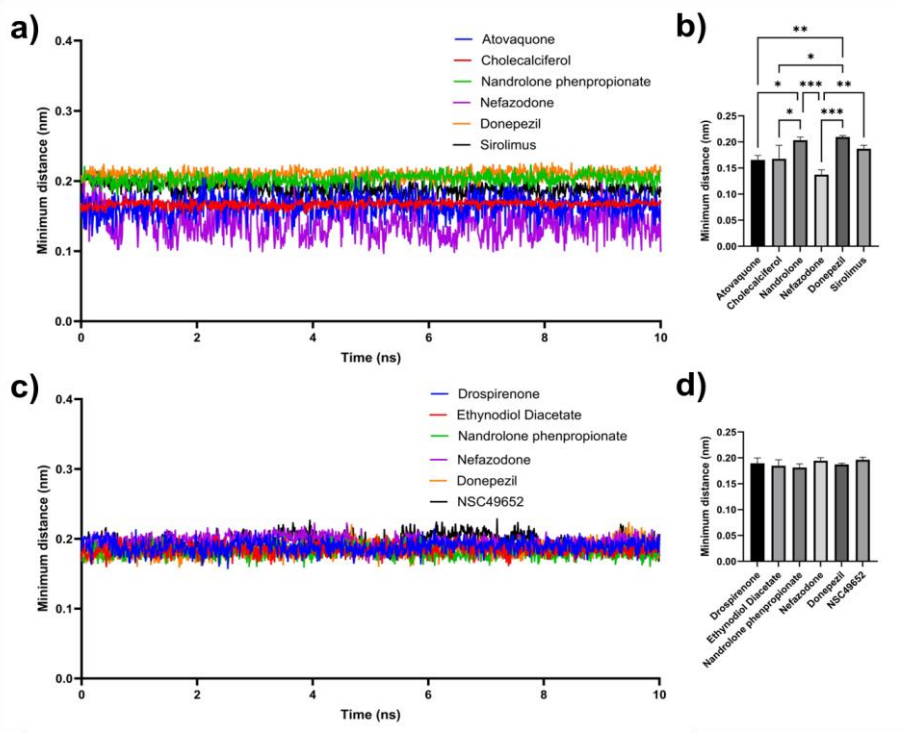

Figure 9. Minimum distance between ligands and proteins in mTOR (1FAP) and p75NTR (3BUK) complexes during 10 ns MD simulations. (a, c) Minimum distance trajectories of 1FAP and 3BUK in complex with selected ligands. (b, d) Average minimum distances values (3–10 ns). Bars represent mean±SD. Statistical significance was determined by one-way ANOVA with Tukey's post-hoc test (*$p < 0.05$, **$p < 0.01$, ***$p < 0.001$), or by Welch's ANOVA with Games–Howell correction when variance homogeneity was violated (e.g., cholecalciferol in mTOR). Absence of asterisks indicates no significant difference.

For the p75NTR complexes (3BUK), drospirenone and ethynodiol diacetate exhibited the most stable dynamic behavior. Protein RMSD values for these complexes remained below 0.07 Å, while ligand RMSD confirmed their stable anchoring. Nandrolone phenpropionate displayed larger deviations (~0.10–0.15 Å), and nefazodone and donepezil showed intermediate stability. The reference agonist NSC49652 also remained stable, validating the simulation protocol (Figure 4c-d).

The RMSF analysis showed minimal perturbation across backbone residues, although nandrolone phenpropionate and donepezil induced slightly higher fluctuations in surface loops compared with drospirenone and ethynodiol diacetate, which displayed the lowest flexibility (Figure 6b). Rg profiles indicated stable receptor compactness around 2.1–2.2 nm across all ligands, with drospirenone showing slightly elevated Rg (~2.7–2.8 nm), suggesting transient global flexibility (Figure 7c-d).

Hydrogen bonding analysis revealed that nefazodone and NSC49652 formed the greatest number of hydrogen bonds (~1.5–2 on average), while drospirenone and ethynodiol diacetate maintained fewer but consistent H-bonds (~0.5–1). Nandrolone phenpropionate displayed irregular hydrogen bonding, consistent with its unstable RMSD (Figure 8c-d). Minimum distance analysis confirmed that all ligands remained in close contact with p75NTR (0.18–0.21 nm), with drospirenone and ethynodiol diacetate maintaining the closest average distances, reinforcing their stable binding conformations (Figure 9c-d).

The MD simulations collectively indicated that atovaquone is the most promising repurposing candidate for mTOR inhibition, while drospirenone and ethynodiol diacetate emerged as the most stable binders for p75NTR. In contrast, nefazodone, despite its strong docking score and hydrogen-bonding capacity, exhibited inconsistent stability across both proteins. The inclusion of sirolimus and NSC49652 as reference ligands further validated the reliability of our docking–MD workflow, while donepezil consistently showed weak binding, confirming its limited relevance for direct targeting of mTOR or p75NTR in AD.

Beyond individual drug performance, our results reveal that the top four candidates for both targets share significant core steroidal or triterpenoid scaffolds, with the exception of atovaquone (a naphthoquinone). This observation aligns with existing literature suggesting that steroid structures are particularly suitable for interacting with growth factors, such as the NGFR [25]. Moreover, steroid-based structures, due to their lipophilicity and ability to cross the blood-brain barrier (BBB), are often considered effective ligands for neurological targets. The intrinsic properties of steroids, including their ability to form multiple hydrophobic and hydrogen bond interactions, make them suitable candidates for binding to receptor proteins such as mTOR and p75NTR. Previous studies have shown that steroids can modulate the activity of growth factors and their receptors, impacting neuronal growth and survival, which are crucial in AD pathology [26].

Importantly, our docking and dynamic stability profiles align with recent MD studies of ligands targeting mTOR and NGFR, which have similarly reported ligand-dependent stabilization of active-site residues and maintenance of conformational compactness [27, 28]. Such concordance reinforces the reliability of our computational approach and supports the pharmacological plausibility of the identified repurposing candidates.

Nevertheless, despite their favorable binding properties, steroid-based drugs are associated with systemic adverse effects–including metabolic disturbances, cardiovascular complications, and immunosuppression–which limit their long-term therapeutic applicability [29]. Future work should therefore focus on structure–activity relationship (SAR) studies and chemical modifications to optimize these scaffolds, aiming to retain therapeutic benefits while minimizing toxicity.

Extended trajectories (≥100 ns) may capture slower conformational modes. Our hardware restricted production runs to 10 ns (with three independent replicas). We mitigated this by analyzing equilibrated windows, applying replicate-based statistics, and benchmarking against reference ligands. Future work will extend simulation times and incorporate free-energy methods as resources permit.

Conclusions

The computational screening identified atovaquone and ethynodiol diacetate as promising candidates for repurposing in AD treatment, specifically targeting mTOR and NGFR, respectively. Their strong binding affinities, favorable pharmacokinetic profiles, and stable molecular interactions with these targets highlight their potential as disease-modifying therapies. Further validation through *in vitro* and

in vivo studies is essential to confirm their therapeutic efficacy and safety, paving the way for clinical trials aimed at addressing the unmet medical needs in AD treatment.

Acknowledgements

This research project is supported by Mae Fah Luang University (Fundamental Fund: fiscal year 2023 by National Science Research and Innovation Fund (NSRF)). (Fundamental Fund: Grant No. 179003/2566).

References

1. Safiri S, Ghaffari Jolfayi A, Fazlollahi A, Morsali S, Sarkesh A, Daei Sorkhabi A, et al. Alzheimer's disease: a comprehensive review of epidemiology, risk factors, symptoms diagnosis, management, caregiving, advanced treatments and associated challenges. Front Med (Lausanne). 2024;11:1474043.
2. Zhang J, Zhang Y, Wang J, Xia Y, Zhang J, Chen L. Recent advances in Alzheimer's disease: Mechanisms, clinical trials and new drug development strategies. Signal Transduct Target Ther. 2024;9(1):211.
3. Hong X, Huang L, Lei F, Li T, Luo Y, Zeng M, et al. The role and pathogenesis of tau protein in Alzheimer's disease. Biomolecules. 2025;15(6):824.
4. Reddi Sree R, Kalyan M, Anand N, Mani S, Gorantla VR, Sakharkar MK, et al. Newer therapeutic approaches in treating Alzheimer's disease: a comprehensive review. ACS Omega. 2025;10(6):5148-71.
5. Xie PL, Zheng MY, Han R, Chen WX, Mao JH. Pharmacological mTOR inhibitors in ameliorating Alzheimer's disease: current review and perspectives. Front Pharmacol. 2024;15:1366061.
6. Perluigi M, Di Domenico F, Butterfield DA. Oxidative damage in neurodegeneration: roles in the pathogenesis and progression of Alzheimer disease. Physiol Rev. 2024;104(1):103-97.
7. Davoody S, Asgari Taei A, Khodabakhsh P, Dargahi L. mTOR signaling and Alzheimer's disease: what we know and where we are? CNS Neurosci Ther. 2024;30(4):e14463.
8. Gao J, Li L. Enhancement of neural regeneration as a therapeutic strategy for Alzheimer's disease (Review). Exp Ther Med. 2023;26(3):444.
9. Bruno F, Abondio P, Montesanto A, Luiselli D, Bruni AC, Maletta R. The nerve growth factor receptor (NGFR/p75^{NTR}): a major player in Alzheimer's disease. Int J Mol Sci. 2023;24(4):3200.
10. Siddiqui T, Cosacak MI, Popova S, Bhattarai P, Yilmaz E, Lee AJ, et al. Nerve growth factor receptor (Ngfr) induces neurogenic plasticity by suppressing reactive astroglial Lcn2/Slc22a17 signaling in Alzheimer's disease. NPJ Regen Med. 2023;8(1):33.
11. Yang CZ, Wang SH, Zhang RH, Lin JH, Tian YH, Yang YQ, et al. Neuroprotective effect of astragalin via activating PI3K/Akt-mTOR-mediated autophagy on APP/PS1 mice. Cell Death Discov. 2023;9(1):15.

12. Chen ZR, Huang JB, Yang SL, Hong FF. Role of cholinergic signaling in Alzheimer's disease. Molecules. 2022;27(6):1816.
13. Cummings JL, Zhou Y, Van Stone A, Cammann D, Tonegawa-Kuji R, Fonseca J, et al. Drug repurposing for Alzheimer's disease and other neurodegenerative disorders. Nat Commun. 2025;16(1):1755.
14. Vicidomini C, Fontanella F, D'Alessandro T, Roviello GN. A survey on computational methods in drug discovery for neurodegenerative diseases. Biomolecules. 2024;14(10):1330.
15. Hassan M, Shahzadi S, Yasir M, Chun W, Kloczkowski A. Computational prognostic evaluation of Alzheimer's drugs from FDA-approved database through structural conformational dynamics and drug repositioning approaches. Sci Rep. 2023;13(1):18022.
16. Bakchi B, Krishna AD, Sreecharan E, Ganesh VBJ, Niharika M, Maharshi S, et al. An overview on applications of SwissADME web tool in the design and development of anticancer, antitubercular and antimicrobial agents: a medicinal chemist’s perspective. J Mol Struct. 2022;1259:132712.
17. Vasanth Kanth TLB, Raha A, Vijay Murali RM, Yuvatha N, Kumaran K, Kirubakaran R, et al. Repurposing of clinically proven bioactive compounds for targeted treatment of Alzheimer's disease using molecular docking approach. In Silico Pharmacol. 2023;11(1):33.
18. Choi J, Chen J, Schreiber SL, Clardy J. Structure of the FKBP12-rapamycin complex interacting with the binding domain of human FRAP. Science. 1996;273(5272):239-42.
19. Gong Y, Cao P, Yu HJ, Jiang T. Crystal structure of the neurotrophin-3 and p75NTR symmetrical complex. Nature. 2008;454(7205):789-93.
20. Morris GM, Huey R, Lindstrom W, Sanner MF, Belew RK, Goodsell DS, et al. AutoDock4 and AutoDockTools4: automated docking with selective receptor flexibility. J Comput Chem. 2009;30(16):2785-91.
21. Lin X, Li X, Lin X. A Review on applications of computational methods in drug screening and design. Molecules. 2020;25(6):1375.
22. Tan C, Jung J, Kobayashi C, Torre DU, Takada S, Sugita Y. Implementation of residue-level coarse-grained models in GENESIS for large-scale molecular dynamics simulations. PLoS Comput Biol. 2022;18(4):e1009578.
23. Hahn DF, Gapsys V, de Groot BL, Mobley DL, Tresadern G. Current state of open source force fields in protein-ligand binding affinity predictions. J Chem Inf Model. 2024;64(13):5063-5076.
24. Guterres H, Im W. Improving protein-ligand docking results with high-throughput molecular dynamics simulations. J Chem Inf Model. 2020 Apr 27;60(4):2189-2198.
25. Iqbal I, Saqib F, Mubarak Z, Latif MF, Wahid M, Nasir B, et al. Alzheimer's disease and drug delivery across the blood-brain barrier: approaches and challenges. Eur J Med Res. 2024;29(1):313.
26. Yilmaz C, Rogdakis T, Latorrata A, Thanou E, Karadima E, Papadimitriou E, et al. ENT-A010, a novel steroid derivative, displays neuroprotective functions and modulates microglial responses. Biomolecules. 2022;12(3):424.

27. Liu Y, Zhang M, Jang H, Nussinov R. The allosteric mechanism of mTOR activation can inform bitopic inhibitor optimization. Chem Sci. 2023;15(3):1003-17.
28. Marafie SK, Alshawaf E, Al-Mulla F, Abubaker J, Mohammad A. Targeting mTOR kinase with natural compounds: potent ATP-competitive inhibition through enhanced binding mechanisms. Pharmaceuticals (Basel). 2024;17(12):1677.
29. Opałka B, Żołnierczuk M, Grabowska M. Immunosuppressive agents-effects on the cardiovascular system and selected metabolic aspects: a review. J Clin Med. 2023;12(21):6935.